Substituent effect on the structural behaviour of modified cyclodextrin: A molecular dynamics study on methylated β-CDs

Wan-Sheung Li, San-Chi Wang, Tsong-Song Hwang and Ito Chao*

Institute of Chemistry, Academia Sinica, Taipei, Taiwan, 11529.

Content of Supplementary Tables and Figures:

Table S9. Calculated correlation coefficients at 1000 ps time frame in the 5000 ps MD simulation of **2c**.

Table S10. Calculated correlation coefficients at 1000 ps time frame in the 5000 ps MD simulation of **3c**.

Table S11. Calculated correlation coefficients of **0a-3a** using 20 ns MD simulations.

Table S12. Calculated correlation coefficients of **1b-3b** using 20 ns MD simulations.

Table S13. Calculated correlation coefficients of **0c-3c** using 20 ns MD simulations.

Table S14. MD simulation results of β-CD (**0a** and **0c**).

Table S15. Calculated energy differences Δ<E> from MD simulations of β-CD (**0a** and **0c**).

Table S16. MD simulations of 6-methyl-β-CD (**1a**-**1c**), 2,6-dimethyl-β-CD (**2a**-**2c**), and 2,3,6-trimethyl-β-CD (**3a**-**3c**) using structures obtained from 3 different initial models.

Table S17. Calculated energy differences Δ<E> from MD simulations of 3 methylated β-CDs (**1**-**3**) from 3 different initial models (*a*-*c*).

Table S18. Correlation analyses of ring tilt of each pyranose ring with $\Delta R_{l\text{-}s}$ of **0a-3a**.

Table S19. Correlation analyses of ring tilt of each pyranose ring with $\Delta R_{l\text{-}s}$ of **1b-3b**.

Table S20. Correlation analyses of ring tilt of each pyranose ring with $\Delta R_{l\text{-}s}$ of **0c-3c**.

Figure S1. The individual ring tilts of the unmethylated **0a** without ring renumbering for the 5000 ps MD.

Figure S2. Population analyses of the titling of the 7 glucose rings of **0a** obtained from sampled structures during 20 ns MD simulations.

Figure S3. Population analyses of the sampled structures obtained from 20 ns MDs with $\Delta R_{l\text{-}s}$ of **0a**-**3a**.

Figure S4. Population analyses of $\Delta R_{l\text{-}s}$ for **0a**-**3a**. Two different starting structures (CSD codes: FAXSUS and DEZMIE10) were used in the 5000 ps MD simulations of **0a**.

Table S1. Calculated correlation coefficients at 1000 ps time frame in the 5000 ps MD simulation of **0a**.

	$\Delta R_{l\text{-}s}$ vs $R_{min}(top)_{sk}$	$\Delta R_{l\text{-}s}$ vs $R_{max}(top)_{sk}$	$\Delta R_{l\text{-}s}$ vs $R_{min}(bot)_{sk}$	$\Delta R_{l\text{-}s}$ vs $R_{max}(bot)_{sk}$
1-5000 ps	-0.15	0.69	-0.72	0.55
1-1000 ps	-0.07	0.67	-0.69	0.45
1001-2000 ps	-0.15	0.69	-0.72	0.63
2001-3000 ps	-0.25	0.58	-0.59	0.31
3001-4000 ps	-0.02	0.77	-0.76	0.68
4001-5000 ps	-0.26	0.70	-0.72	0.47

Table S2. Calculated correlation coefficients at 1000 ps time frame in the 5000 ps MD simulation of **1a**.

	$\Delta R_{l\text{-}s}$ vs $R_{min}(top)_{sk}$	$\Delta R_{l\text{-}s}$ vs $R_{max}(top)_{sk}$	$\Delta R_{l\text{-}s}$ vs $R_{min}(bot)_{sk}$	$\Delta R_{l\text{-}s}$ vs $R_{max}(bot)_{sk}$
1-5000 ps	-0.34	0.44	-0.38	0.14
1-1000 ps	-0.43	0.44	-0.41	0.17
1001-2000 ps	-0.29	0.46	-0.38	0.15
2001-3000 ps	-0.32	0.40	-0.32	0.10
3001-4000 ps	-0.33	0.48	-0.33	0.06
4001-5000 ps	-0.31	0.45	-0.45	0.24

Table S3. Calculated correlation coefficients at 1000 ps time frame in the 5000 ps MD simulation of **2a**.

	$\Delta R_{l\text{-}s}$ vs $R_{min}(top)_{sk}$	$\Delta R_{l\text{-}s}$ vs $R_{max}(top)_{sk}$	$\Delta R_{l\text{-}s}$ vs $R_{min}(bot)_{sk}$	$\Delta R_{l\text{-}s}$ vs $R_{max}(bot)_{sk}$
1-5000 ps	-0.37	0.54	-0.53	0.29
1-1000 ps	-0.35	0.55	-0.56	0.37
1001-2000 ps	-0.45	0.58	-0.53	0.20
2001-3000 ps	-0.37	0.53	-0.45	0.29
3001-4000 ps	-0.33	0.56	-0.55	0.37
4001-5000 ps	-0.28	0.43	-0.48	0.17

Table S4. Calculated correlation coefficients at 1000 ps time frame in the 5000 ps MD simulation of **3a**.

	$\Delta R_{l\text{-}s}$ vs $R_{min}(top)_{sk}$	$\Delta R_{l\text{-}s}$ vs $R_{max}(top)_{sk}$	$\Delta R_{l\text{-}s}$ vs $R_{min}(bot)_{sk}$	$\Delta R_{l\text{-}s}$ vs $R_{max}(bot)_{sk}$
1-5000 ps	-0.47	0.60	-0.53	0.24
1-1000 ps	-0.41	0.52	-0.49	0.28
1001-2000 ps	-0.37	0.53	-0.42	0.11
2001-3000 ps	-0.55	0.68	-0.60	0.31
3001-4000 ps	-0.52	0.59	-0.58	0.25
4001-5000 ps	-0.39	0.59	-0.43	0.13

Table S5. Calculated correlation coefficients at 1000 ps time frame in the 5000 ps MD simulation of **1b**.

	$\Delta R_{l\text{-}s}$ vs $R_{min}(top)_{sk}$	$\Delta R_{l\text{-}s}$ vs $R_{max}(top)_{sk}$	$\Delta R_{l\text{-}s}$ vs $R_{min}(bot)_{sk}$	$\Delta R_{l\text{-}s}$ vs $R_{max}(bot)_{sk}$
1-5000 ps	-0.45	0.54	-0.47	0.37
1-1000 ps	-0.31	0.49	-0.42	0.24
1001-2000 ps	-0.43	0.52	-0.32	0.26
2001-3000 ps	-0.49	0.43	-0.47	0.37
3001-4000 ps	-0.45	0.57	-0.51	0.36
4001-5000 ps	-0.46	0.66	-0.52	0.54

Table S6. Calculated correlation coefficients at 1000 ps time frame in the 5000 ps MD simulation of **2b**.

	$\Delta R_{l\text{-}s}$ vs $R_{min}(top)_{sk}$	$\Delta R_{l\text{-}s}$ vs $R_{max}(top)_{sk}$	$\Delta R_{l\text{-}s}$ vs $R_{min}(bot)_{sk}$	$\Delta R_{l\text{-}s}$ vs $R_{max}(bot)_{sk}$
1-5000 ps	-0.58	0.54	-0.44	0.30
1-1000 ps	-0.45	0.57	-0.31	0.27
1001-2000 ps	-0.60	0.50	-0.44	0.25
2001-3000 ps	-0.50	0.53	-0.29	0.16
3001-4000 ps	-0.59	0.46	-0.44	0.21
4001-5000 ps	-0.68	0.60	-0.61	0.44

Table S7. Calculated correlation coefficients at 1000 ps time frame in the 5000 ps MD simulation of **3b**.

	$\Delta R_{l\text{-}s}$ vs $R_{min}(top)_{sk}$	$\Delta R_{l\text{-}s}$ vs $R_{max}(top)_{sk}$	$\Delta R_{l\text{-}s}$ vs $R_{min}(bot)_{sk}$	$\Delta R_{l\text{-}s}$ vs $R_{max}(bot)_{sk}$
1-5000 ps	-0.49	0.62	-0.22	0.35
1-1000 ps	-0.56	0.67	-0.10	0.29
1001-2000 ps	-0.55	0.69	-0.35	0.34
2001-3000 ps	-0.44	0.59	-0.08	0.18
3001-4000 ps	-0.46	0.58	-0.33	0.47
4001-5000 ps	-0.44	0.63	-0.07	0.40

Table S8. Calculated correlation coefficients at 1000 ps time frame in the 5000 ps MD simulation of **1c**.

	$\Delta R_{l\text{-}s}$ vs $R_{min}(top)_{sk}$	$\Delta R_{l\text{-}s}$ vs $R_{max}(top)_{sk}$	$\Delta R_{l\text{-}s}$ vs $R_{min}(bot)_{sk}$	$\Delta R_{l\text{-}s}$ vs $R_{max}(bot)_{sk}$
1-5000 ps	-0.55	0.71	-0.49	0.37
1-1000 ps	-0.57	0.71	-0.49	0.36
1001-2000 ps	-0.53	0.65	-0.53	0.38
2001-3000 ps	-0.63	0.76	-0.43	0.40
3001-4000 ps	-0.48	0.71	-0.50	0.28
4001-5000 ps	-0.50	0.73	-0.52	0.37

Table S9. Calculated correlation coefficients at 1000 ps time frame in the 5000 ps MD simulation of **2c**.

	$\Delta R_{l\text{-}s}$ vs $R_{min}(top)_{sk}$	$\Delta R_{l\text{-}s}$ vs $R_{max}(top)_{sk}$	$\Delta R_{l\text{-}s}$ vs $R_{min}(bot)_{sk}$	$\Delta R_{l\text{-}s}$ vs $R_{max}(bot)_{sk}$
1-5000 ps	-0.58	0.68	-0.54	0.20
1-1000 ps	-0.63	0.68	-0.49	0.22
1001-2000 ps	-0.54	0.64	-0.53	0.11
2001-3000 ps	-0.60	0.68	-0.49	0.09
3001-4000 ps	-0.56	0.74	-0.60	0.36
4001-5000 ps	-0.51	0.64	-0.48	0.15

Table S10. Calculated correlation coefficients at 1000 ps time frame in the 5000 ps MD simulation of **3c**.

	$\Delta R_{l\text{-}s}$ vs $R_{min}(top)_{sk}$	$\Delta R_{l\text{-}s}$ vs $R_{max}(top)_{sk}$	$\Delta R_{l\text{-}s}$ vs $R_{min}(bot)_{sk}$	$\Delta R_{l\text{-}s}$ vs $R_{max}(bot)_{sk}$
1-5000 ps	-0.53	0.70	-0.51	0.12
1-1000 ps	-0.51	0.73	-0.54	0.28
1001-2000 ps	-0.54	0.69	-0.42	0.00
2001-3000 ps	-0.55	0.68	-0.49	0.20
3001-4000 ps	-0.45	0.69	-0.47	-0.05
4001-5000 ps	-0.62	0.70	-0.60	0.10

Table S11. Calculated correlation coefficients of **0a-3a** using 20 ns MD simulations.

	0a	1a	2a	3a
$\Delta R_{l\text{-}s}$ vs $R_{min}(top)_{sk}$	-0.26	-0.33	-0.39	-0.47
$\Delta R_{l\text{-}s}$ vs $R_{max}(top)_{sk}$	0.70	0.50	0.57	0.59
$\Delta R_{l\text{-}s}$ vs $R_{min}(bot)_{sk}$	-0.76	-0.46	-0.55	-0.57
$\Delta R_{l\text{-}s}$ vs $R_{max}(bot)_{sk}$	0.64	0.22	0.29	0.26

Table S12. Calculated correlation coefficients of **1b-3b** using 20 ns MD simulations.

	1b	2b[a]	3b
$\Delta R_{l\text{-}s}$ vs $R_{min}(top)_{sk}$	-0.58	-0.54	-0.48
$\Delta R_{l\text{-}s}$ vs $R_{max}(top)_{sk}$	0.73	0.27	0.52
$\Delta R_{l\text{-}s}$ vs $R_{min}(bot)_{sk}$	-0.57	-0.18	-0.40
$\Delta R_{l\text{-}s}$ vs $R_{max}(bot)_{sk}$	0.33	0.06	0.42

[a] one of the glucose rings flipped upside down at ~9500 ps into the simulation.

Table S13. Calculated correlation coefficients of **0c-3c** using 20 ns MD simulations.

	0c	1c	2c	3c
$\Delta R_{l\text{-}s}$ vs $R_{min}(top)_{sk}$	-0.61	-0.50	-0.54	-0.57
$\Delta R_{l\text{-}s}$ vs $R_{max}(top)_{sk}$	0.54	0.61	0.69	0.71
$\Delta R_{l\text{-}s}$ vs $R_{min}(bot)_{sk}$	-0.68	-0.52	-0.47	-0.45
$\Delta R_{l\text{-}s}$ vs $R_{max}(bot)_{sk}$	0.57	0.37	0.25	0.08

Table S14. MD simulation results of β-CD (**0a** and **0c**).[a,b]

kJ/mol	**0a**	**0c**
Av. PE scaled to 300K	749.08	772.66
Av. $\langle E \rangle_{stretch}$	206.83	207.18
Av. $\langle E \rangle_{bend}$	317.63	320.69
Av. $\langle E \rangle_{torsion}$	558.39	553.63
Av. $\langle E \rangle_{vdw}$	-14.08	-16.33
Av. $\langle E \rangle_{electrostatic}$	-183.55	-141.36
Av. $\langle E \rangle_{solvation\ 1}$	11.03	11.07
Av. $\langle E \rangle_{solvation\ 2}$	-147.18	-162.23

[a] Simulations were carried out with 200 ps equilibration step followed by 5000 ps MD at 300 K in a continuum water solvation model using AMBER* force field.

[b] Energy from the simulation of β-CD in conformation *b* is similar to that in **c** due to the configuration of the $^{O}S_2$ pyranose ring is changed to $^{1}C_4$ during the equilibration step. Constraints were also applied to the $^{O}S_2$ ring (with a force constant of 500 kJ/mol) but the ring still changed to $^{1}C_4$ during the equilibration step.

Table S15. Calculated energy differences Δ<E> from MD simulations of β-CD (**0a** and **0c**).

kJ/mol	Δ<E> **0a-0c**
$\Delta\langle E \rangle_{total}$	-23.58
$\Delta\langle E \rangle_{stretch}$	-0.35
$\Delta\langle E \rangle_{bend}$	-3.06
$\Delta\langle E \rangle_{torsion}$	4.76
$\Delta\langle E \rangle_{vdw}$	2.25
$\Delta\langle E \rangle_{electrostatics}$	-42.19
$\Delta\langle E \rangle_{solvation}$	15.01

Table S16. MD simulations of 6-methyl-β-CD (**1a-1c**), 2,6-dimethyl-β-CD (**2a-2c**), and 2,3,6-trimethyl-β-CD (**3a-3c**) using structures obtained from 3 different initial models.[a]

	Ordered ($^4\mathbf{C_1}$)[b]			Disordered ($^o\mathbf{S_2}$)[c]			Disordered ($^1\mathbf{C_4}$)[d]		
kJ/mol	**1a**	**2a**	**3a**	**1b**	**2b**	**3b**	**1c**	**2c**	**3c**
Av. PE scaled to 300K	951.27	1366.95	1639.11	998.68	1423.09	1672.22	979.65	1393.95	1647.08
Av. $\langle E \rangle_{stretch}$	234.86	265.18	289.06	235.20	265.86	297.56	235.58	265.83	297.75
Av. $\langle E \rangle_{bend}$	357.83	410.32	458.91	361.11	413.43	458.80	364.86	414.99	460.05
Av. $\langle E \rangle_{torsion}$	531.52	493.60	500.77	536.37	513.68	518.68	529.45	497.34	504.55
Av. $\langle E \rangle_{vdw}$	-5.28	10.48	26.12	-3.01	11.66	25.44	-6.77	8.04	22.02
Av. $\langle E \rangle_{electrostatic}$	-61.70	282.32	439.22	-16.16	326.37	456.05	-24.03	321.48	451.31
Av. $\langle E \rangle_{solvation\ 1}$	28.02	43.78	51.48	27.63	42.54	51.52	26.58	42.18	52.48
Av. $\langle E \rangle_{solvation\ 2}$	-133.99	-138.73	-135.44	-142.45	-150.45	-135.83	-146.03	-155.91	-141.09

[a] Simulations were carried out with 200 ps equilibration step followed by 5000 ps MD at 300 K in a continuum water solvation model.

[b] Structures obtained from crystal structure of 2,6-dimethyl- β CD complex (CSD code: DEZME10).

[c] Structures obtained from crystal structure of 2,3,6-trimethyl- β CD (CSD code: GELKEN10)

[d] Structures obtained from crystal structure of 2,3,6-trimethyl- β CD (CSD code: HEZWAK01)

Table S17. Calculated energy differences Δ<E> from MD simulations of 3 methylated β-CDs (**1-3**) from 3 different initial models (*a-c*)

	Me- β -CD **1**			DM-β-CD **2**			TM-β-CD **3**		
kJ/mol	Δ<E>**1a-1c**	Δ<E>**1a-1b**	Δ<E>**1c-1b**	Δ<E>**2a-2c**	Δ<E>**2a-2b**	Δ<E>**2c-2b**	Δ<E>**3a-3c**	Δ<E>**3a-3b**	Δ<E>**3c-3b**
Δ<E>total	-28.38	-47.41	-19.03	-27.00	-56.14	-29.14	-7.97	-33.11	-25.14
Δ<E>stretch	-0.72	-0.34	0.38	-0.65	-0.68	-0.03	-8.69	-8.5	0.19
Δ<E>bend	-7.03	-3.28	3.75	-4.67	-3.11	1.56	-1.14	0.11	1.25
Δ<E>torsion	2.07	-4.85	-6.92	-3.74	-20.08	-16.34	-3.78	-17.91	-14.13
Δ<E>vdw	1.49	-2.27	-3.76	2.44	-1.18	-3.62	4.1	0.68	-3.42
Δ<E>electrostatics	-37.67	-45.54	-7.87	-39.16	-44.05	-4.89	-12.09	-16.83	-4.74
Δ<E>solvation	13.48	8.85	-4.63	18.78	12.96	-5.82	4.65	0.35	-4.30

Table S18. Correlation analyses of ring tilt of each pyranose ring with $\Delta R_{l\text{-}s}$ of **0a-3a**.

	0a	1a	2a	3a
G1	0.16	-0.09	-0.04	-0.18
G2	0.18	0.24	0.26	0.32
G3	-0.30	-0.12	-0.14	-0.11
G4	-0.36	-0.16	-0.24	-0.25
G5	0.26	0.08	0.14	0.09
G6	-0.14	0.12	0.12	0.19
G7	-0.61	-0.27	-0.37	-0.35

The glucose rings of each sampled structure are renumbered by first measuring the longest opposite glycosidic O…O distances and this distance is defined as the elliptic long axis. Then the rings are renumbered according to diagram as shown below in a clockwise direction (by viewing the cyclodextrin structure from the top rim to the bottom rim). The ring tilt is defined as the angle between the two least square mean planes of the glucose ring (defined by C_2, C_3, C_5 and O_5) and the glycosidic mean plane (defined by the 7 glycosidic O-atoms).

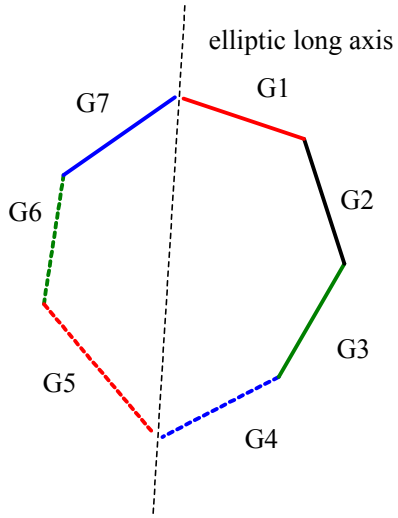

Table S19. Correlation analyses of ring tilt of each pyranose ring with $\Delta R_{l\text{-}s}$ of **1b-3b**.

	1b	2b	3b
G1	-0.04	-0.11	-0.08
G2	0.26	0.39	0.24
G3	-0.09	-0.20	-0.06
G4	-0.32	-0.27	-0.24
G5	0.33	0.29	0.32
G6	-0.04	0.02	-0.01
G7	-0.15	-0.08	-0.02

Table S20. Correlation analyses of ring tilt of each pyranose ring with $\Delta R_{l\text{-}s}$ of **0c-3c**.

	0c	1c	2c	3c
G1	0.10	-0.18	-0.11	-0.18
G2	0.46	0.36	0.34	0.26
G3	-0.35	0.09	-0.16	-0.01
G4	-0.37	-0.33	-0.35	-0.34
G5	0.22	0.22	0.30	0.25
G6	-0.05	0.23	0.35	0.33
G7	-0.49	-0.46	-0.33	-0.28

Figure S1. The individual ring tilts of the unmethylated **0a** without ring renumbering for the 5000 ps MD.

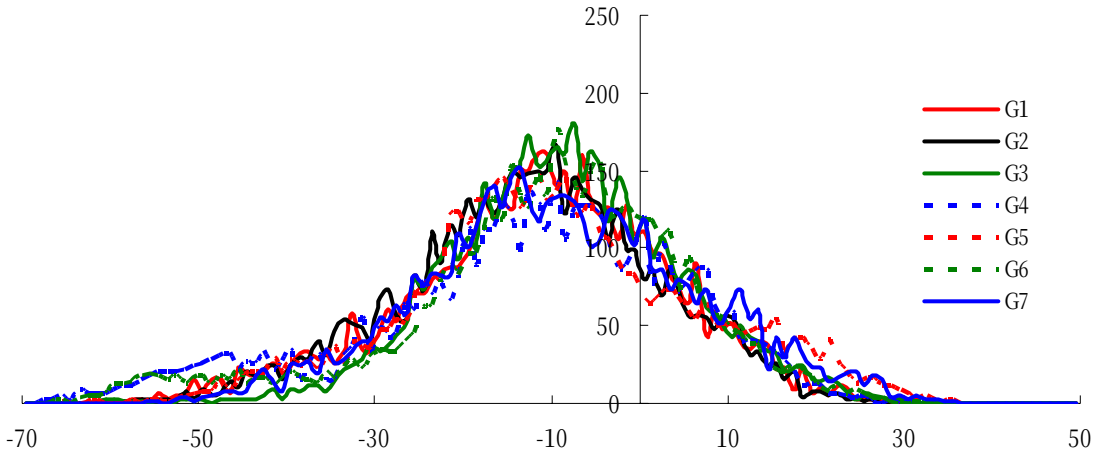

Figure S2. Population analyses of the titling of the 7 glucose rings of **0a** obtained from sampled structures during 20 ns MD simulations.

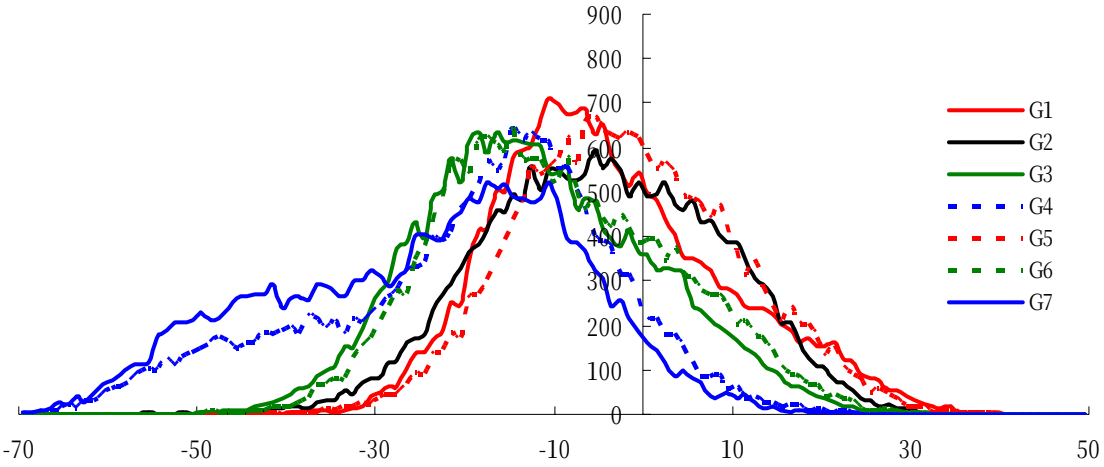

Figure S3. Population analyses of the sampled structures obtained from 20 ns MDs with $\Delta R_{l\text{-}s}$ of **0a-3a**.

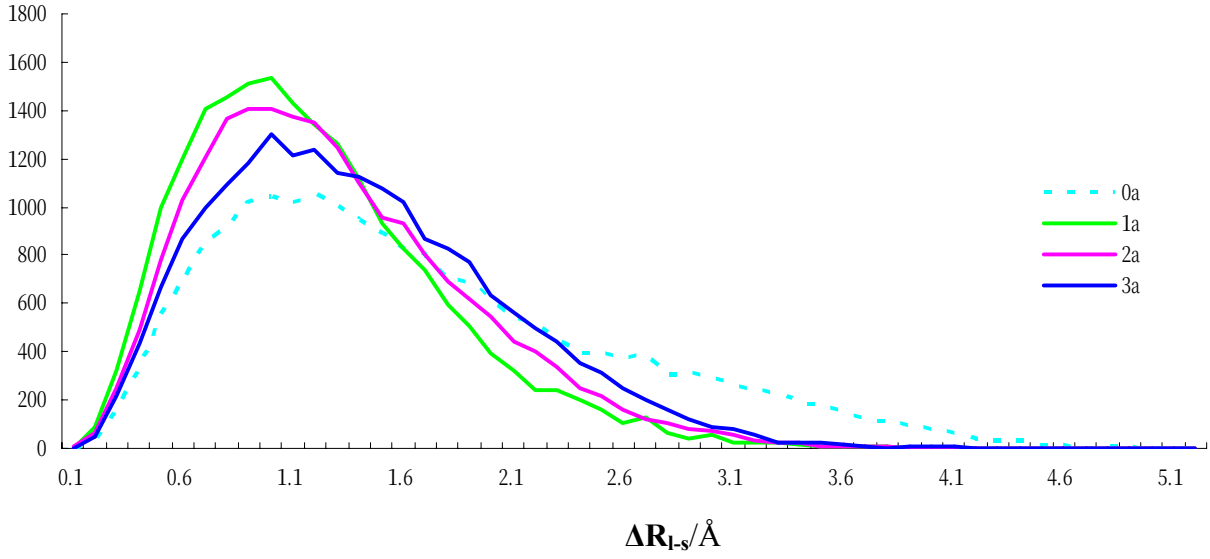

Figure S4. Population analyses of $\Delta R_{l\text{-}s}$ for **0a-3a.** Two different starting structures (CSD codes: FAXSUS and DEZMIE10) were used in the 5000 ps MD simulations of **0a**.